Nuclear Materials and Energy 9 (2016) 353–359

Contents lists available at ScienceDirect

Nuclear Materials and Energy

journal homepage: www.elsevier.com/locate/nme

Strength anisotropy of rolled 11Cr-ODS steel

Takashi Tanno*, Yasuhide Yano, Hiroshi Oka, Satoshi Ohtsuka, Tomoyuki Uwaba, Takeji Kaito

Japan Atomic Energy Agency, 4002 Narita-cho Oarai-machi, Higashiibaraki-gun, 311-1393, Ibaraki, Japan

ARTICLE INFO

Article history:
Received 23 October 2015
Revised 12 January 2016
Accepted 23 February 2016
Available online 1 April 2016

Keywords:
Oxide dispersion strengthened steel
Creep rupture
Prior particle boundary
Ti-rich precipitate

ABSTRACT

Materials for core components of fusion reactors and fast reactors, such as blankets and fuel cladding tubes, must offer the best possible high temperature strength and irradiation resistance because they will be exposed to high heat flux and heavy neutron irradiation. Japan Atomic Energy Agency (JAEA) has been developing 9 and 11 chromium (Cr) oxide dispersion strengthened (ODS) steels as candidate materials for advanced fast reactor cladding tubes. In this study the JAEA 11Cr-ODS steel was rolled in order to evaluate its anisotropy. The tensile tests and creep tests were carried out at 700 °C in longitudinal and transverse orientations. The anisotropy of the tensile strength was negligible, though that of the creep strength was distinct. The observation results and chemical composition mapping suggested that the cause of the anisotropy in the creep strength was a previously formed columnar boundary, that is, a prior particle boundary including Ti-rich sub-micro metric precipitates.

1. Introduction

The blankets of fusion reactors and the fuel cladding tubes of advanced fast reactors will be exposed to heavy neutron irradiation and high heat flux at high temperature. The materials for these components must have not only high irradiation resistance but also superior high temperature strength for durability. Oxide dispersion strengthened (ODS) steels have been developed as a promising candidate material for these components [1–5].

In Japan Atomic Energy Agency (JAEA), 9Cr tempered martensitic ODS steel has been developed for cladding tubes of advanced fast reactors. The material offers superior properties, such as high temperature strength [6,7]. From the viewpoint of the compatibility with a fuel reprocessing process, however, it is also important to study other candidate materials offering better corrosion resistance, e.g. relatively high-Cr ODS tempered martensitic steels. The addition of at least 11–12 wt% Cr appreciably improves the corrosion resistance of steels. However, it is difficult to keep the tempered martensite matrix the same as that of the high performance 9Cr-ODS steel when Cr content exceeds 11–12 wt%. JAEA has been developing the 11Cr-ODS steel as the material which offers better corrosion resistance as well as the other good properties of 9Cr-ODS steel. Though the addition of higher Cr could decrease ductility and toughness, JAEA 11Cr-ODS steel achieved good impact properties by adoption of the pre-alloy fabrication process without any elemental powder which can suppress formation of inclusions [8].

High performance ODS steels are certainly good materials for fusion reactors and fast reactors. However not only consolidated bulk materials but also rolled plate or tube materials are necessary to assemble the components. It is important to evaluate the anisotropy of rolled ODS steels, because rolled materials generally have anisotropic structure and strength. The anisotropy in the tensile properties of 9Cr-ODS cladding tubes fabricated in CEA was reported [9]. According to that study, the anisotropy in the tensile properties and textures could be made slight with an appropriate heat treatment. The anisotropy of creep strength should be evaluated from various aspects. But studies focusing on the anisotropy of ODS steels are insufficient. In this study, the JAEA pre-alloy 11Cr-ODS steel was rolled, and mechanical tests, structural observations and fractography were carried out in order to evaluate the anisotropy. Then the relationships between the anisotropy of strength and structures were discussed.

2. Experimental procedure

2.1. Material

The 11Cr-ODS steel lots “15P” (0.2Ti) and “17P” (0.3Ti) were used in this work. Both lots were fabricated by the pre-alloy

* Corresponding author.
E-mail address: tanno.takashi@jaea.go.jp (T. Tanno).

http://dx.doi.org/10.1016/j.nme.2016.02.009

Table 1
Chemical compositions of 11Cr-ODS steel at each fabrication stage in this work.

Lot	Stage	Chemical composition (wt%)															
		Fe	C	Si	Mn	P	S	Ni	Cr	W	Ti	Y	O	N	Ar	Y_2O_3[a]	Ex.O[b]
15P	Raw powder	Bal.	0.14	0.04	0.04	0.003	0.002	0.43	11.04	1.31	0.24	–	0.021	0.003	0.0001	–	–
	MAed powder	Bal.	0.14	0.04	0.04	<0.005	0.002	0.39	10.91	1.32	0.22	0.27	0.125	0.004	0.0037	0.34	0.05
	Extruded bar	Bal.	0.14	0.04	0.05	<0.005	0.003	0.40	10.82	1.28	0.22	0.27	0.133	0.006	0.004	0.34	0.06
17P	Raw powder	Bal.	0.13	0.04	0.04	<0.005	0.002	0.40	10.80	1.30	0.28	–	0.023	0.002	0.0003	–	–
	MAed powder	Bal.	0.13	0.04	0.04	<0.005	0.001	0.40	10.91	1.27	0.28	0.27	0.132	0.004	0.0047	0.34	0.06
	Extruded bar	Bal.	0.13	0.04	0.04	0.005	0.002	0.40	10.90	1.30	0.28	0.27	0.138	0.004	0.005	0.34	0.07

[a] Calculated from Y content with the assumption that Y is present as Y_2O_3.
[b] Defined as the value obtained by subtracting oxygen content as Y_2O_3 from the total O content in the steel.

process without any elemental powder which adjusts chemical composition. The process can considerably reduce the formation of inclusions. In the pre-alloy process, only the Ar-gas atomized alloy powder and Y_2O_3 powder were mechanically alloyed (MAed) by an attritor type ball-mill with ultra-high purity Ar (99.9999 wt%) gas atmosphere. The MAed powders were canned and evacuated to 1.3×10^{-3} Pa at 400 °C. The vacuum condition was kept for over 4 h, then the cans were sealed completely. They were pre-heated for over 3 h at 1150 °C followed by hot extrusion (HE). The chemical compositions of the atomized raw powders, MAed powders, and extruded bars are as shown in Table 1. This table indicates that the major chemical compositions did not change significantly in any processes. The oxygen increase during the MA was 0.034–0.039 wt% (340–390 wppm) except for the oxygen composing Y_2O_3, and the increase through the HE process was 60–80 wppm. The extruded cylindrical bars were finished by normalizing-and-tempering (NT), i.e. 1050 °C annealing for 1 h (austenitizing) followed by air-cooling (AC), and 800 °C annealing for 1 h followed by AC. After these heat treatment, the 11Cr-ODS steel bar was composed by major matrix phase of the tempered martensite and a few 10% of residual α ferrite phase similar to 9Cr-ODS steels [8]. The residual α ferrite phase is respectively harder than the tempered martensite, and it seems to roll as a reinforcement phase [7]. Some of the bars were rolled by 3-stage cold rolling. The annealing at 1050 °C for 1 h was carried out in order to soften the bars, prior to a 45% cold rolling, in each stage. The triply rolled plates were finished by the NT heat treatment.

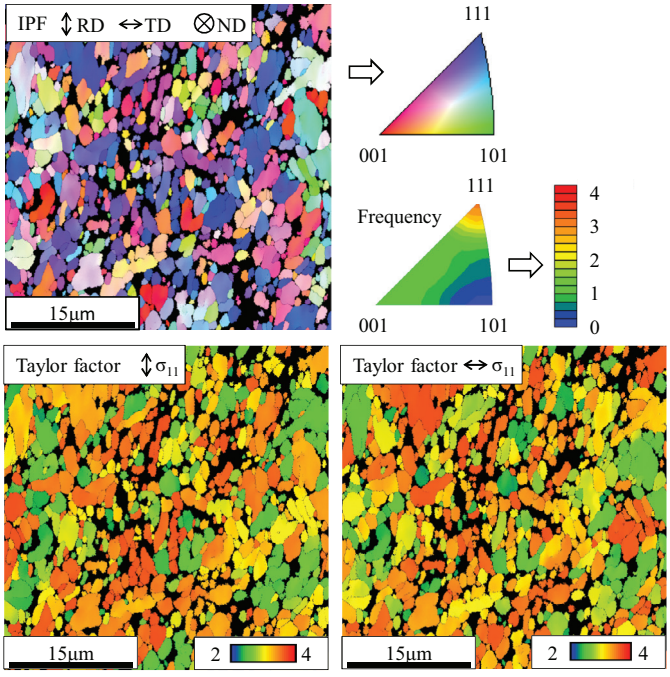

Fig. 1. Inverse pole figure map (upper) and Taylor factor maps (lower) obtained by EBSD analysis. RD is the rolling direction, TD is the transvers direction and ND is the normal direction opposite the rolled plane. The principal stress (σ_{11}) axis paralleled to RD (left) and TD (right) in the analysis.

2.2. Mechanical tests

Tensile tests and creep tests were carried out. Two types of specimens were used in this work, one was a cylindrical bar type and the other was a miniature plate type made from the rolled plate. The cylindrical bar type specimens were machined from the NT heat treated bars. The plate type specimens were cut from the NT heat treated plates by the electro-discharge method. All of the specimens were finished by polishing along the loading direction. The plate type specimens were selected in the longitudinal (L) orientation which was paralleled to the rolling direction and in the transverse (T) orientation in order to evaluate the anisotropy.

The cylindrical bar tensile specimens had a 30.0 mm gauge length and 6.0 mm diameter. The size of the SS-3 miniature tensile test specimen was adopted for the plate type specimens. The gauge region had a 7.62 mm length, 1.52 mm width and 0.76 mm thickness. The tensile tests were carried out at 700 °C in air. The strain rate for the cylindrical bar specimens was 5.0×10^{-5} s^{-1} until 0.2% yield, and then it was changed to 1.25×10^{-3} s^{-1}. The strain rate for plate specimens was constant at 8.33×10^{-4} s^{-1}. The total elongation was evaluated by measuring the change of the specimen length.

The cylindrical bar creep specimens had a 32.0 mm gauge length and 6.0 mm diameter. The miniature creep test specimen was adopted for the plate type specimens. The gauge region had a 12.0 mm length, 2.0 mm width and 1.0 mm thickness. The creep tests were carried out at 700 °C in air, and the stress range was 140–200 MPa.

2.3. Structure observations and fractography

The micro-structure observations were carried out in order to confirm the features of the rolled plates. Fractography and cross section observations of tested plate specimens were carried out in order to evaluate the difference of fracture mechanism in the L-orientation and T-orientation. The specimens for micro-structure and cross section observations were prepared by embedding into a resin, and finished by mirror-like polishing. In this work, several apparatuses were used: a scanning electron microscope (SEM; Hitachi S3400N), an orientation image microscopy system (OIM; TSL solutions) for electron backscatter diffraction (EBSD) analysis, energy dispersive X-ray spectrometer (EDS; EDAX Apollo-X) and electron probe micro-analyzer (EPMA; JEOL JXA-8500F).

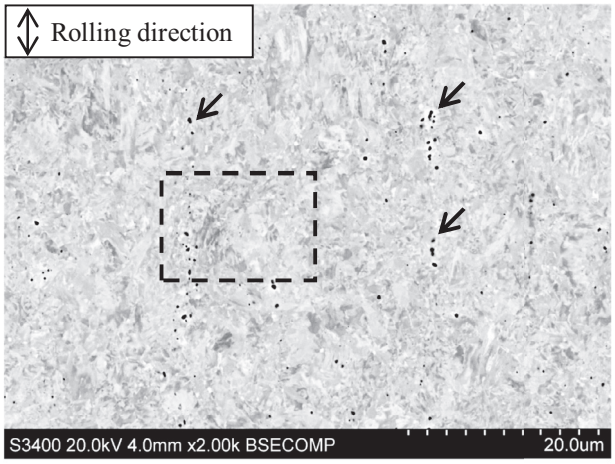

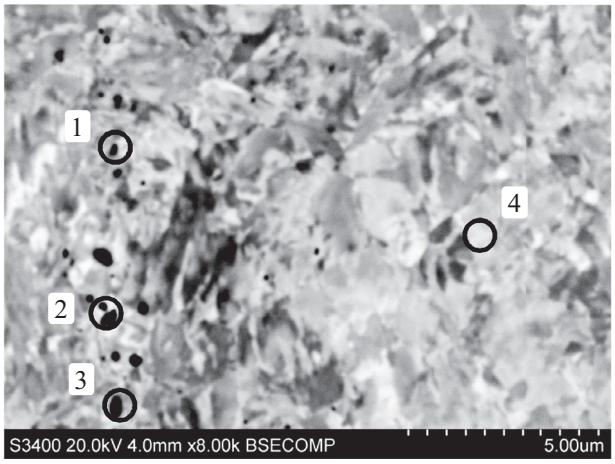

No.	Cr	W	Ti	Y	(wt%)
1	12.2	3.0	1.8	0.9	Prec.
2	11.9	3.2	5.3	0.6	Prec.
3	11.0	3.1	5.2	0.9	Prec.
4	11.7	2.4	0.2	0.7	Matrix

Fig. 2. Microstructure observations of the rolled 11Cr-ODS steel 15P. Lower is magnified image of the area indicated by dotted rectangle in upper image. The table lists the EDS results of spot analysis at the circles.

3. Results

3.1. Structure of rolled ODS steel

The results of EBSD analysis corresponding to rolled 15P plate is shown in Fig. 1. The shape of grains was generally equiaxial and the diameter was up to a few micro meter. The oriented texture owing to the rolling was observed. The $<111>$ direction tended to orient to normal direction opposite the rolled plane. However, Taylor factor maps for each principal stress (σ_{11}) axis along rolling direction and transvers direction were nearly equal. The results of EBSD analysis corresponding to rolled 17P plate was almost the same as 15P. Thus it is considered that the rolled texture could not cause any anisotropy in tensile properties.

Ti-rich sub-micro metric precipitates were lined up along the rolling direction as shown in Fig. 2. The sub-micro metric precipitates were hardly observed in columnar regions between the lines. The lines in 17P were observed more clearly, and the number of the lines was also larger than that in 15P. Since these features were almost the same as those in reported for cylindrical bar specimens [8], it was considered that the columnar structure including the

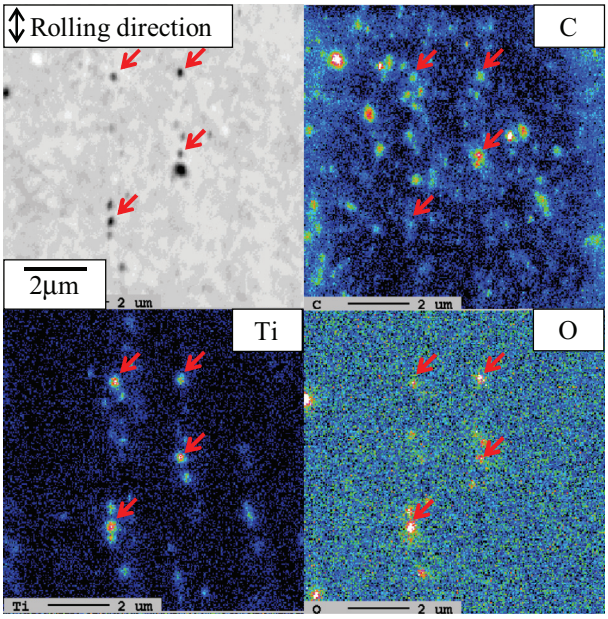

Fig. 3. Chemical composition map of the rolled 11Cr-ODS steel 15P obtained by EPMA.

lined up Ti-rich sub-micro metric precipitates, which had formed in the extruded cylindrical bar, remained after rolling.

The precipitates images overlapped the areas with concentrations of Ti, O and C, in the chemical composition maps obtained by EPMA as shown in Fig. 3. The Ti-rich sub-micro metric precipitates seemed to be complexes of oxides and carbides. In addition, some precipitates included nitrogen. The results of SEM observations and EPMA analysis indicated that the Ti-rich sub-micro metric precipitates were formed on a previously existing powder particle boundary, that is, a prior particle boundary (PPB). Oxidation and Ti segregation could occur in the vicinity of the surface of the MAed powder particles by residual slight air in the cans during pre-heating at 1150 °C. The Ti-oxides would be the initiation sites of precipitations of oxides and/or carbides in the following heat treatment. According to previous research, Ti segregation and precipitates could form creep voids leading to creep rupture [10]. It was also reported that the PPB in ODS steels could affect creep behavior [11]. Since the PPB features in 17P were more prominent than those in 15P, the PPB influence would be larger for higher Ti content.

3.2. Mechanical tests

The anisotropy of ultimate tensile strength (UTS) at 700 °C was negligibly small as shown in Fig. 4. The UTS of the rolled plate specimens nearly equaled to that of the cylindrical bar specimens; therefore, the size effects of specimens were also negligible. Although the total elongation in the T-orientation was smaller than that in the L-orientation, both of them were over 20%. The difference between the behaviors of 15P and 17P was indistinct. Therefore the influence of Ti content on tensile properties did not seem to be significant in the range of 0.2–0.3 wt%. The difference between the total elongation in the L-orientation of the cylindrical bar specimens and plate specimens might be a size effect. In the case of a large specimen, the inner stress of the specimen could increase rapidly after necking, because the stress state changes from uniaxial to triaxial due to deformation constraining by its own volume. In other word, the state come closer to a plane strain condition. On the other hand, the inner stress of a small specimen could not increase significantly, even if necking occur, be-

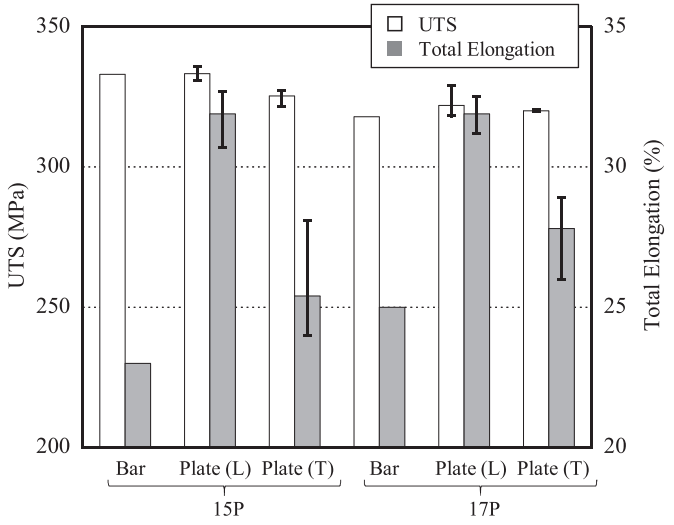

Fig. 4. Results of tensile tests of 11Cr-ODS steel for each shape and orientation at 700 °C.

cause the small volume cannot constrain the deformation, and the stress state transient is slight. As a result, tensile deformation voids would form in the larger cylindrical bar specimen more than that in the smaller plate specimen. Therefore many voids in the larger bar specimen could link earlier and decrease the total elongation of it.

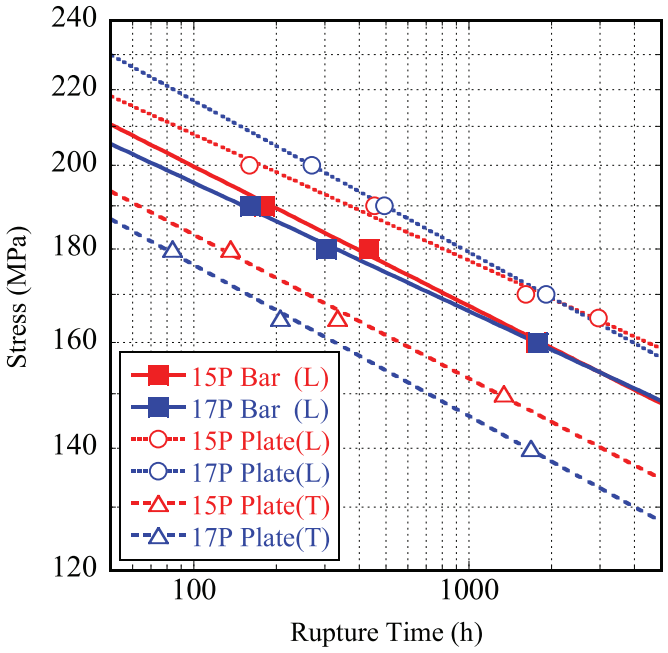

Fig. 5. Results of creep rupture tests of 11Cr-ODS steel for each shape and orientation at 700 °C.

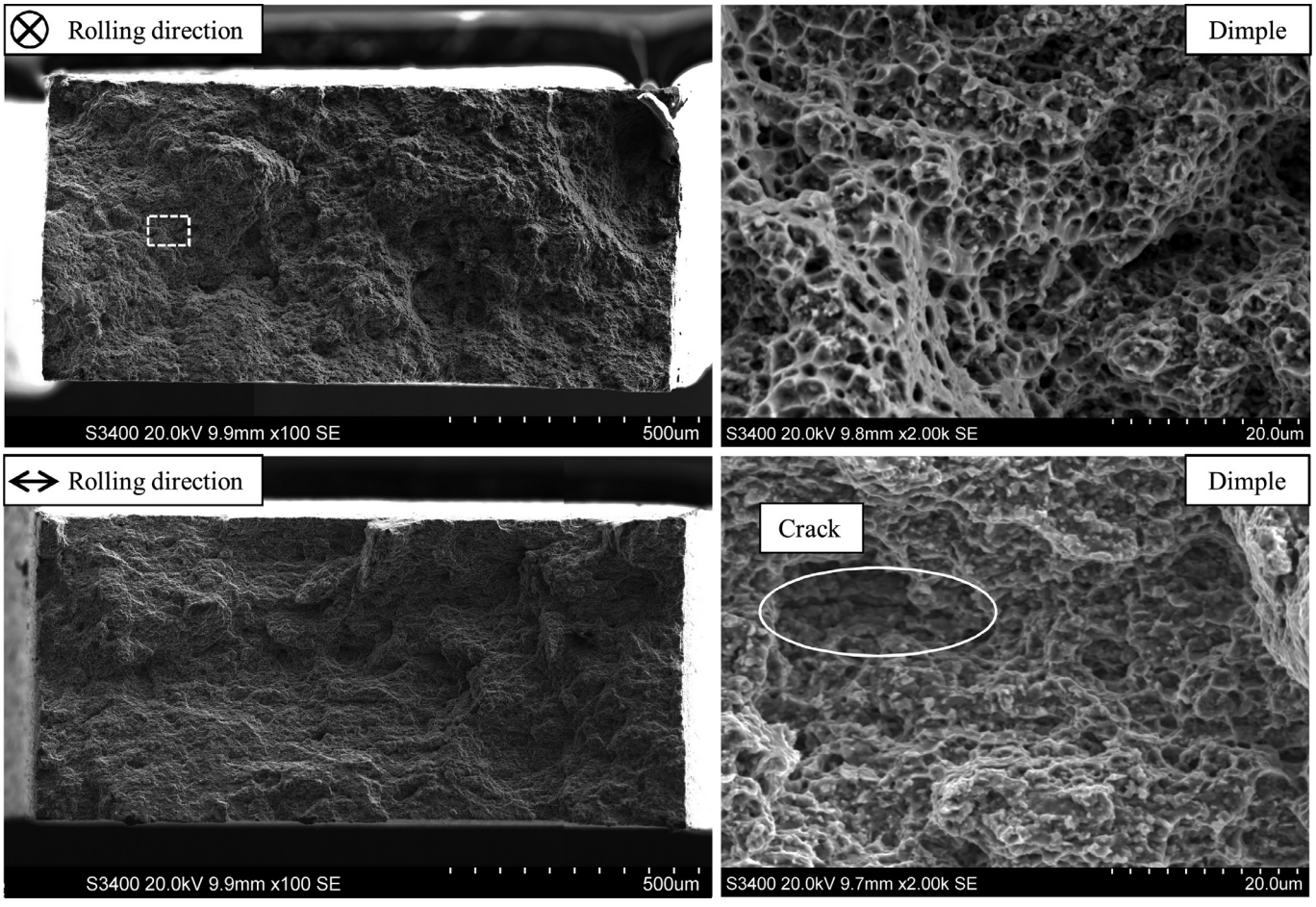

Fig. 6. Macro (left) and micro (right) fractures of rolled 11Cr-ODS steel 15P after tensile tests at 700 °C in L-orientation (upper) and T-orientation (lower).

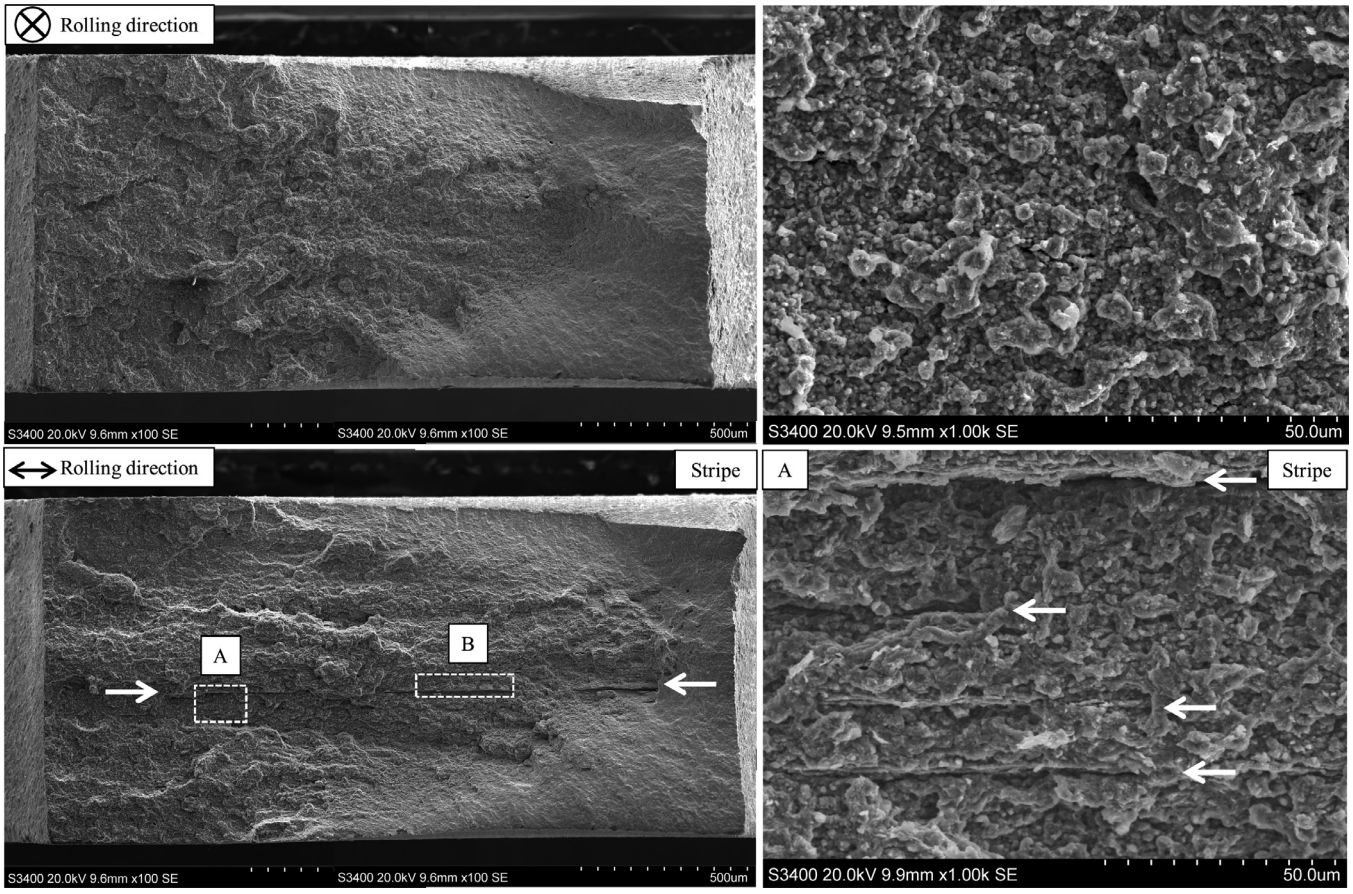

Fig. 7. Macro (left) and micro (right) fractures of rolled 11Cr-ODS steel 15P after creep tests at 700 °C in L-orientation (upper: 170 MPa) and T-orientation (lower: 150 MPa). Tilted fracture of area "B" is shown in Fig. 7.

The anisotropy of creep strength of the rolled plate specimens was clear as shown in Fig. 5. The creep strength in the T-orientation was smaller than that in the L-orientation. The creep strength of 17P in the T-orientation was lower than that of 15P, but the creep strength in the L-orientation did not depend on Ti content. These results indicated that the Ti increase caused degradation of the creep strength in the T-orientation and enhanced the anisotropy. The difference between the creep strength in the L-orientation of cylindrical bar and plate specimens might be a result of a distribution change of the lined up Ti-rich sub-micro metric precipitates owing to rolling. The stress state change could be not dominant, because the reduction of area in creep tests was up to a few percent, though that of the cylindrical bar spesimens in tensile tests reached 40%.

3.3. Fractography

3.3.1. Tensile specimens

Fig. 6 shows the fractures of the miniature plate specimens in the L and T-orientations after the tensile tests. The fractures in both orientations were ductile morphology. The fracture of the L-orientation was completely covered with fine dimples. Not only dimples but also cracks along rolling direction were observed for the T-orientation fracture. The cracks would be initiated at PPBs because of the orientation of the cracks.

3.3.2. Creep specimens

Fig. 7 shows the macro-fracture of the miniature plate creep specimens after the creep tests. Noticeable stripes up to 1 mm in length along the rolling direction were observed on the fractures of the specimens in only the T-orientation. The stripes were steps containing a sub-structure as shown in Fig. 8. Fine Ti-rich particles and very fine stripes along the rolling direction were observed on the rising face of the step. The Ti-rich particles mean that the rising face should be a PPB including Ti-rich sub-micro metric precipitates. And the fine strips mean that slips were repeated on the rising face, that is, the PPB. Therefore massive slips would occur on the PPBs during the T-orientation creep tests.

Other large scale steps were observed in the cross sections of only the T-orientation specimens as shown in Fig. 9. Their height was 10–100 μm, and the edges of the steps were peeling off. The Ti-precipitates were lined up along the rolling direction from the root of the peeled tip. The features observed in the cross sections indicate that the PPB should be a massive break interface in the T-orientation creep rupture.

4. Discussion

In this work, the major structural feature of the rolled plates was the PPB including lined up Ti-rich sub-micro metric precipitates. The relationships between anisotropic structure characterized by the PPB and strength anisotropy are discussed in the following.

4.1. Anisotropy in the tensile property of rolled ODS steel

The fracture modes in tensile tests in both L and T-orientations at 700 °C were ductile. The grains can deform by a dislocation

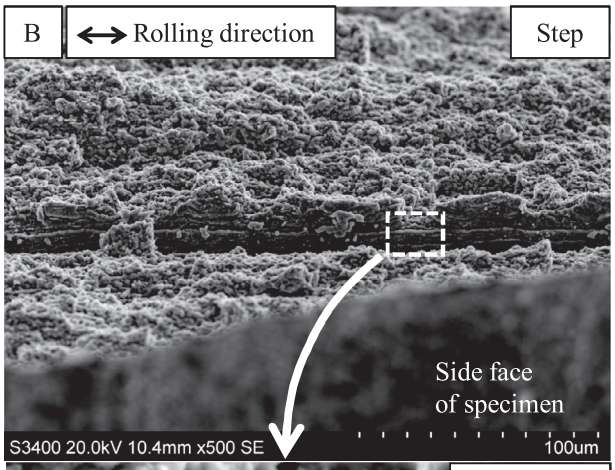

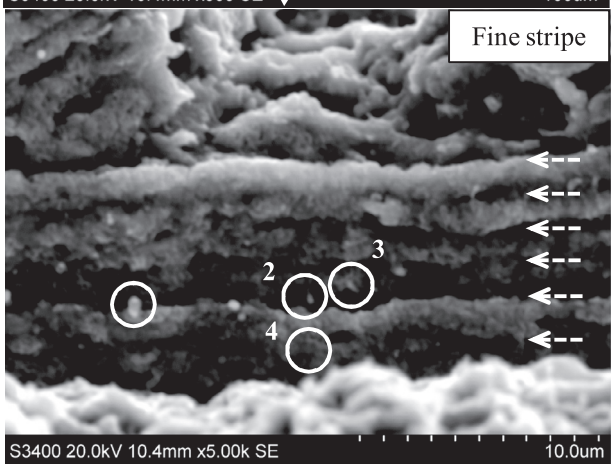

No.	Cr	W	Ti	Y	(wt%)
1	12.9	2.3	1.2	0.2	Particle
2	11.3	1.6	1.1	0.3	Particle
3	12.9	2.0	1.5	0.2	Particle
4	11.1	1.6	0.4	0.3	Matrix

Fig. 8. Tilted fracture of area "B" in Fig. 7. Circles and dotted arrows indicate Ti-rich sub-micro metric particles and fine stripes, respectively. The table in this figure lists the results of EDS analysis at the circles.

gliding mechanism, because the tensile strength was higher than the threshold stress (~200 MPa) against dispersion strengthening [12]. Therefore the tensile strength should depend on the properties of the grains rather than the influence of the PPB. That would be the reason why the anisotropy in the tensile strength was negligible.

The anisotropy of total elongation should be related to the difference of fractures. The cracks along rolling direction, which seemed to be PPBs, were observed only in the T-orientation. The PPB is the interface where the bonding strength is weaker than other boundaries including common grain boundary. Thus the PPBs would be crack initiation sites, and the total elongation in the T-orientation would be lower than that in the L-orientation.

4.2. Anisotropy in the creep strength of rolled ODS steel

The grains of 11Cr-ODS steel are highly strengthened by nano-sized oxide particles, which retard deformation caused by dislocation motion at high temperature. Therefore, the creep deformation mechanism must be a grain boundary slip which might be assisted by a diffusion. The PPB is a boundary where grain boundaries are in a meta-stable state in a column. Fracture initiation on the PPB could preferentially take place by either slipping or detachment.

The PPB has hardly any effect on properties in the L-orientation, because most of the PPBs are parallel to the loading direction. Even if cracking occurs on the PPB at the end of a column, the propagation will be stopped at the edge of the column. As a result, the creep strength in the L-orientation will be dominated by a "normal" creep deformation and rupture mechanism: grain boundary slip, creep void formation and linkage between them as shown in Fig. 10.

On the other hand, the PPB is considered to affect properties in the T-orientation. The massive slips occur on the PPBs, and the strain is concentrated at PPB triple-junctions. Then cracking or separating occurs at the PPB triple-junctions. The cracks or separations can broadly and continuously propagate on neighboring PPBs as shown in Fig. 10. As a result, the creep strength in the T-orientation will be affected by the massive slip and crack propagation on the PPB. That is considered to be the reason for early rupture and strength degradation in the T-orientation.

Higher Ti content will induce larger creep strength anisotropy, because the PPB is characterized by Ti precipitation.

5. Conclusion

Rolled JAEA pre-alloy 11Cr-ODS steel plates were fabricated. Tensile tests, creep rupture tests, micro-structure observations and fractography were carried out in order to evaluate the relationships between the anisotropy in the micro-structure and strength. The origin of the strength anisotropy was discussed from the view point of the anisotropic features of the micro-structure. The following points were obtained in this work.

(1) Ti-rich sub-micro metric precipitates were lined up along the rolling direction which was parallel to the extrusion direction. They were complexes of oxides and carbides. The Ti-rich sub-micro metric precipitates should be formed on the prior powder boundary (PPB). The PPB was considered to be formed by oxidation on the surface of the mechanical alloyed powder during pre-heating before hot-extrusion of the cylindrical bar.
(2) The anisotropy in the tensile strength at 700 °C was negligibly small. The creep strength at 700 °C in the transverse (T) orientation was lower than that in the longitudinal (L) orientation. The anisotropy of creep strength tended to be larger with larger Ti content.
(3) The rupture mode in tensile tests at 700 °C in the L and T-orientations were ductile. Therefore the tensile strength would be dominated by the property of the grains rather than the PPB, and the anisotropy was negligible.
(4) The fracture after the creep test at 700 °C in the T-orientation differed from that in the L-orientation. Steps where massive slips occurred at the PPB were observed only in the T-orientation fracture. In addition, massive break away on the PPB was also observed in the cross section of the T-orientation specimens. Thus the PPB should cause creep strength degradation in the T-orientation, that is, the anisotropy. Higher Ti content could enhance the anisotropy, because the PPB was characterized by Ti precipitation.

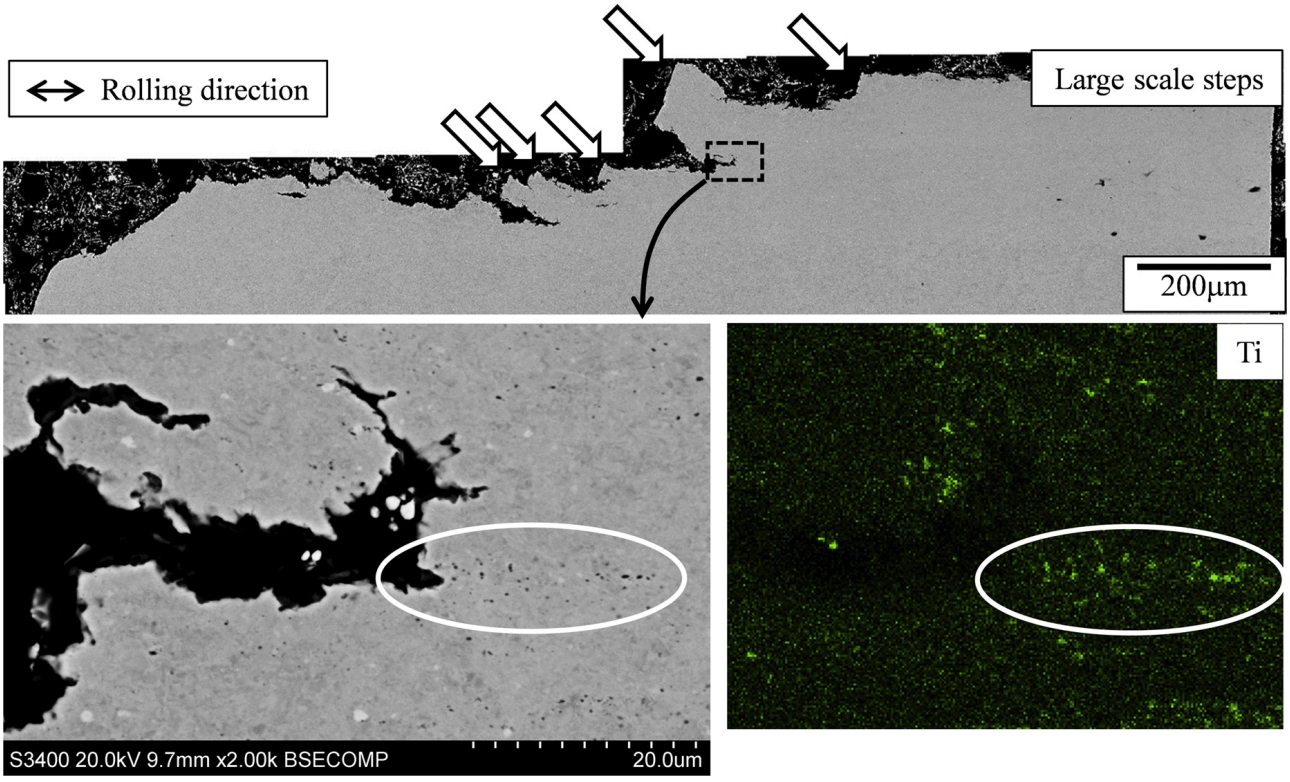

Fig. 9. Macro (upper) and micro (lower) cross section of rolled 11Cr-ODS steel 17P after creep tests at 700 °C and 140 MPa. The white allows indicate large scale steps which seem to have been formed by a massive break on the PPBs. The circle indicates lined up Ti-rich sub-micro metric precipitates.

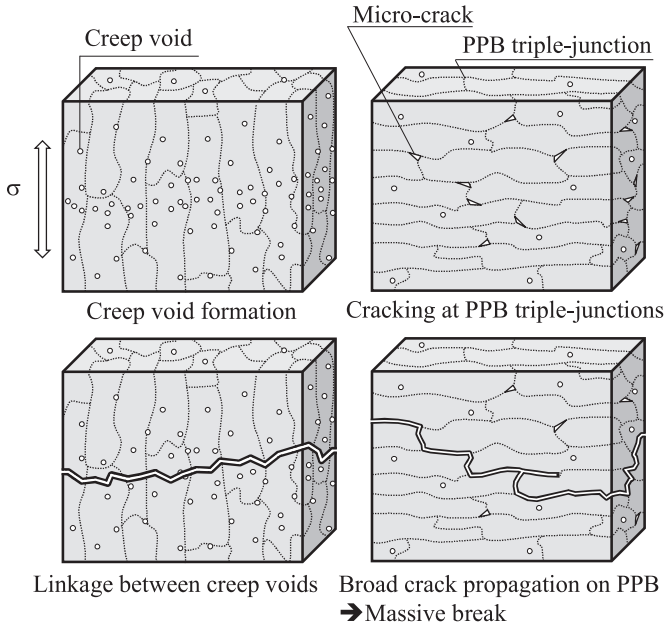

Fig. 10. Schematic creep rupture mechanisms of rolled ODS steel including columnar PPB (dotted lines) in the L-orientation (left) and the T-orientation (right) based on the results of observations in this work.

Acknowledgments

The authors are pleased to thank Dr. M. Fujiwara and Mr. T. Nakai, of the Kobelco Research Institute (KRI) for useful advice and fruitful discussions throughout the work. The authors are grateful to Mr. Y. Amano of KRI for the EPMA analysis. The authors are also pleased to thank Mr. S. Sato of JAEA for making the tensile tests. Finally, the authors are pleased to thank Dr. H. Kurishita who retired from Tohoku University for fruitful discussions about deformation and rupture.

References

[1] G.R. Romanoski, L.L. Snead, R.L. Klueh, D.T. Hoelzer, J. Nucl. Mater. 283-287 (2000) 642–646.
[2] D. Stork, P. Agostini, J.L. Boutard, D. Buckthorp, E. Diegele, S.L. Dudarev, C. English, G. Federici, M.R. Gilbert, S. Gonzalez, A. Ibarra, Ch. Linsmeier, A. Li Puma, G. Marbach, P.F. Morris, L.W. Packer, B. Raj, M. Rieth, M.Q. Tran, D.J. Ward, S.J. Zinkle, J. Nucl. Mater. 455 (2014) 277–291.
[3] Y. de Carlan, J.-L. Bechade, P. Dubuisson, J.-L. Seran, P. Billot, A. Bougault, T. Cozzika, S. Doriot, D. Hamon, J. Henry, M. Ratti, N. Lochet, D. Nunes, P. Olier, T. Leblond, M.H. Mathon, J. Nucl. Mater. 386-388 (2009) 430–432.
[4] Y. Shimakawa, S. Kasai, M. Konomura, M. Toda, Nucl. Technol. 140 (2002) 1–17.
[5] S. Ukai, M. Fujiwara, J. Nucl. Mater. 307-311 (2002) 749–757.
[6] S. Ukai, S. Ohtsuka, T. Kaito, H. Sakasegawa, N. Chikata, S. Hayashi, Mater. Sci. Eng. A 510-511 (2009) 115–120.
[7] T. Narita, S. Ukai, S. Ohtsuka, M. Inoue, J. Nucl. Mater. 417 (2011) 158–161.
[8] T. Tanno, S. Ohtsuka, Y. Yano, T. Kaito, Y. Oba, M. Ohnuma, S. Koyama, K. Tanaka, J. Nucl. Mater. 440 (2013) 568–574.
[9] L. Toualbi, C. Cayron, P. Olier, R. Loge, Y. de carlan, J. Nucl. Mater. 442 (2013) 410–416.
[10] R.L. Klueh, J.P. Shingledecker, R.W. Swindeman, D.T. Hoelzer, J. Nucl. Mater. 341 (2005) 103–114.
[11] H. Sakasegawa, S. Ukai, M. Tamura, S. Ohtsuka, H. Tanigawa, N. Nucl. Mater. 373 (2008) 82–89.
[12] T. Tanno, S. Ohtsuka, Y. Yamo, T. Kaito, K. Tanaka, J. Nucl. Mater. 455 (2014) 480–485.